Indian Journal of Fibre & Textile Research
Vol. 45, March 2020, pp. 72-79

Water filtration using nonwoven cartridge filter system

Rahul Gadkari, Bipin Kumar[a], Wazed Ali, Apurba Das & R Alagirusamy
Department of Textile & Fibre Engineering, Indian Institute of Technology Delhi, New Delhi 110 016, India

Received 19 December 2018; revised received and accepted 6 February 2019

A cartridge based fibrous filtration system has been designed and investigated. For the fibrous medium, needle-punch nonwoven structure has been selected and different nonwoven samples are analysed for the water purification. A series of different needle-punched nonwovens made of polypropylene have been produced by changing mass per unit area, needling density and fibre linear density. A chemical oxygen demand test has been employed to obtain the filtration efficiency (FE). The FE obtained for these samples ranges from 8.84% to 78.04% in purifying the reference water (mud water). It has been found that the FE increases with increase in mass per unit area and needling density ($p < 0.01$). Also, the filter media made of finer fibres displays higher FE than coarser fibre ($p < 0.01$). On examining the filter performance in multiple filtration cycles, it is found that the FE increases initially and finally reaches to a saturation value. A good correlation ($r^2 > 0.95$) has been found for the FE of each cycle with the air permeability, thickness and weight density of the loaded filter. The FE of the bare nonwoven (maximum FE) further improves (95%) by incorporating activated particles.

Keywords: Chemical oxygen demand, Fibrous filter, Nonwovens, Needle-punched fabric, Polypropylene

1 Introduction

In a recent data from World Bank, more than half of the world population lives in rural areas. Most of these people do not have adequate access to clean water, and their prime source of reservoir come from either pond or underground water. Because of extreme poverty or limited electricity, they are not able to afford advance filtration modalities for purifying water such as electrodeionization, reverse osmosis, UV radiation, nano-fibrous filtration, ion exchange and distillation[1]. Surely, it would be of great support if we can provide them a simple, efficient and cheap water filtration system.

Filtration using fibrous filter media has been proven to be one of the effective techniques utilized for the purification of air or fluid[2,3]. They can be either woven or nonwoven in construction[4,5]. A nonwoven is a random array of fibres having interconnecting pores throughout the cross-section. The nonwoven filter media has high filtration efficiency, more availability of pores per unit area, good cake discharge property, low cost and easy production[6]. Typically, a nonwoven media is able to remove particles within the range 1−1000 nm. Different nonwoven types including melt blown, electrospun, spun laced, wet spun and needle-punched are being used for filtration in many industrial applications related to food and beverage, pharmaceutical, oils, solvents, biotech, water, acid and bases[7-9]. Among all nonwovens, nano-fibrous web usually produced via electrospun or melt spun show greater advantage and potential in filtration. However, the production cost has always been an issue for producing nano-filters on commercial scale. Nevertheless, the needle-punched nonwoven is a cheap alternative and commercially more successful[10]. Furthermore, the needle-punch production technology nowadays is more mature, and allows easy means to get optimized structure by changing material and processing, including fibre characteristic, feed rate, layering factor, needle type and punching attributes. In this study, it is preferred to use needle-punch samples for the development of cartridge filter.

Several impurities including hazardous chemicals, biological contaminants, suspended solids, oils and gases may present in the contaminated water. Especially in remote villages, the rain water is harvested into a pond, and used by local people. The major content is the suspended particles of clay or mud in the pond water. In this work, we are mainly targeting for the filtration of pond water. There are several mechanisms for the particle capture in a nonwoven including sieving, interception, and impaction or through diffusion. The particle retention is highly dependent on the porous architecture of the

[a]Corresponding author.
E-mail: bipin@iitd.ac.in

fibrous material[9, 11-14]. So, the pore size and its distribution in the nonwoven structure are the key factors in any filter development. Several material and structural parameters such as fibre denier, mass density, and needle density can influence pore distribution, and the understanding of their roles on filtration can be useful for design optimization.

With the above facts in mind, the filtration performance of different porous networks has been first examined in this study. Several cartridge filters are produced using different nonwovens produced by varying processing parameter. Important structural factors, i.e. mass density, needling density and fibre denier, are critically examined for their effect on the filtration. The filtration efficiency is obtained using a newly designed experimental set-up.

2 Materials and Methods

2.1 Needle-punched Nonwoven

A series of 9 nonwoven samples was manufactured using a needle-punched nonwoven machine (DILO), consisting of opener; card, cross lapper, and needle loom. All the samples were made from 100% polypropylene fibres (fibre length 51mm). Two different fibre densities (denier), viz 2.5 den and 6 den, were used for production. Some machine parameters including feed rate and needle punching frequency were altered to vary structural characteristics, i.e. mass per unit area (g/m^2) and needling density (punches/m^2). Two levels of needling density (210×10^4, 225×10^4 punches/m^2) and three levels of mass per unit area (400, 500 and 600 g/m^2) were obtained. Table 1 shows the structural details of all produced samples.

2.2 Cartridge Formation

The cartridge filter media was prepared by wrapping the nonwoven filter on an open porous tube. The diameter and the length of the tube were 2.2 cm and 20.5 cm respectively [Fig. 1(a)]. At first, the nonwoven filter media of width 20.5 cm was cut and then it was tightly wrapped around the tube [Fig. 1(b)]. The end of the nonwoven filter was fused on the sample itself to make the whole specimen compact. An annular cap with inner diameter equal to porous tube diameter was used to seal the upper and lower end.

2.3 Instrument Set-up for Filtration

A simple set-up was designed and developed to do the water filtration [Fig. 1(d)]. The set-up mainly consists of three main components, namely an input can to store impure water, a mouth/opening which holds the filter cartridge and a collector. The input can is used to supply the impure water (unfiltered) to the

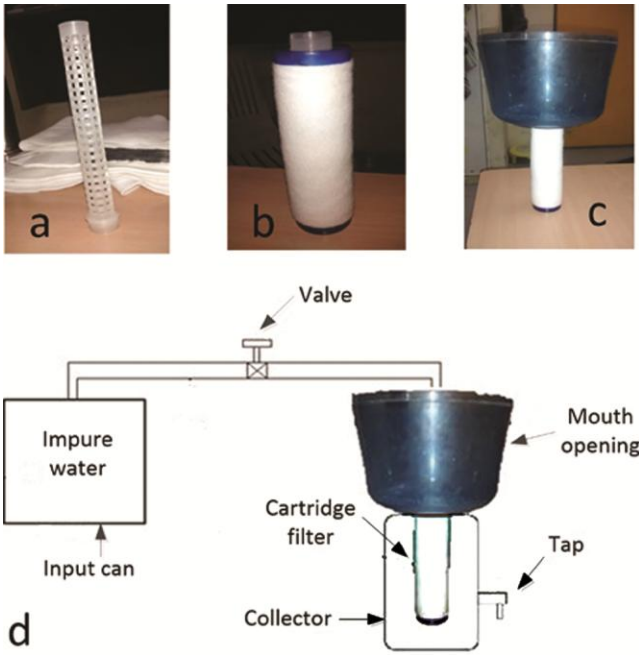

Fig. 1 — Photographs of (a) porous tube on which filter media is wound, (b) nonwoven filter cartridge, (c) attachment of cartridge with a bucket, and (d) schematic of the set-up used for filtration test

Table 1 — Details of nonwoven filter samples
[Fibre – Polypropylene, shape factor of fibre − 0.715, and fibre length − 51mm]

Sample code	Fibre denier	Mass per unit Area, g/m^2	Needling density$\times10^4$ punches/m^2	Thickness (t_o), mm	Porosity (ε_{fo})
F1	2.5	400	210	2.89	0.85
F2	2.5	500	210	3.36	0.84
F3	2.5	600	210	3.60	0.82
F4	2.5	400	225	3.18	0.87
F5	2.5	500	225	3.88	0.86
F6	2.5	600	225	3.91	0.84
F7	6	400	225	3.74	0.89
F8	6	500	225	4.24	0.88
F9	6	600	225	4.33	0.85

cartridge specimen. A steel pipe is used to connect the can with the cartridge using a valve attachment. An open plastic bucket is used to hold the filter cartridge [Fig. (1c)]. A hole of 2.2 cm diameter is punctured at the bottom of bucket to fit the cartridge tube. The bottom of the tube is completely sealed to avoid any free flow of water. The collector is used to cover the cartridge system, and collect the filtrate (filtered water). An opening is created to its side to collect the filtrate in a test tube, and used for further analysis.

2.4 Testing Procedure

2.4.1 Filtration Efficiency

The filtration efficiency (FE) of the nonwoven filter was measured using COD (chemical oxygen demand) testing of the impure (unfiltered) and filtered water. The COD determines the amount of oxygen required for the chemical oxidation of organic matter present in the waste water[15]. It measures the oxygen equivalent (mL) consumed by organic matter per liter of water sample during strong chemical oxidation. The impure water sample was prepared using mud that was mixed properly in the tap water (COD value 64 mg/L). A fixed amount of the mud (100 g/L of water) was used for the slurry.

A closed reflux method was used to determine the COD of water samples. A 2.5 mL of filtered water was placed in a culture testing tube followed by addition of 1.5 mL of reagent potassium dichromate ($K_2Cr_2O_7$). Then, a fixed amount (3.5 mL) of the sulphuric acid (H_2SO_4) was added inside the tube so that acid layer is formed under sample-digestion solution layer. The final solution was mixed thoroughly. Finally, the testing tube was placed in a block digester at 150° C and refluxes the sample for straight 2 h behind a protective shield. After the refluxing, the titration was done using ferrous ammonium sulphate (FAS) solution until the end point where the color is changed from blue-green to reddish brown is reached. The amount of FAS solution required to complete titration was recorded. The COD can be calculated using the following equation:

$$\text{COD (mg of } O_2/\text{L)} = \frac{(A-B)\times M\times 8000}{V} \quad \ldots (2)$$

where *A* is the volume of FAS (mL) used for filtered water; *B*, the volume of FAS (mL) needed for the distilled water; *M*, the molarity of FAS solution (0.1 moles/L); and *V*, the volume of water used (2.5 mL). Similar method was followed to obtain the COD for unfiltered water which was fixed in our case (204.8 mg/L). Based on the COD values of unfiltered and filtered water, the filtration efficiency (FE) was calculated using the following relationship:

$$\text{FE (\%)} = \frac{\text{COD}_{\text{unfiltered}} - \text{COD}_{\text{filtered}}}{\text{COD}_{\text{unfiltered}}} \times 100 \quad \ldots (2)$$

2.4.2 Porometry Test

The pore characteristics were obtained by porometric analysis using a porometer (Model: POROLUX^{TM} 500). A circular sample was cut and put in a tray containing porefil which is used as a wetting liquid (ASTM F 316-03). Once the sample was completely wet, then the inert gas was passed through it to replace the liquid. The flow rate of gas and the corresponding pressure required to displace the liquid were continuously obtained. Some useful pore characteristics including smallest pore size (SFP), mean flow pore size (MFP) and pore pressures were obtained.

2.4.3 Air Permeability

The air permeability of the nonwoven was measured using a TEXTEST air permeability tester (Model: FX330) at 98 Pa pressure. It is expressed as cc/cm^2/s, indicating the volume rate of the air passage through a unit area of specimen at a fixed pressure difference.

2.5 Theoretical Background

In general, there are two groups for characterization of nonwoven filters[11]. First method is to take the account of structural measurements like mean pore size and air permeability. The second group relates to the dynamic changes in the FE and flow resistance. The flux equation is found to be useful to examine dynamic behavior, as shown below:

$$J = \frac{\Delta P}{\mu R} \quad \ldots (3)$$

where J is the permeate flux (m^3/m^2/s); ΔP, the transmembrane pressure (Pa); μ, the permeate viscosity (Pa.s); and R, the flow resistance (m^{-1}). In the present case, we conducted the test in batches where a fixed amount of filtered water (500 mL) was collected in each filtration cycle, and the COD value was measured. Figure 2 shows the schematic of the formation of cake layer and depth filtration after each cycle. As more cycles are conducted, the porous network will change which may influence the filtration performance. Herein, we are not bothered about the filtration time but on the quality of the filtered water in each cycle.

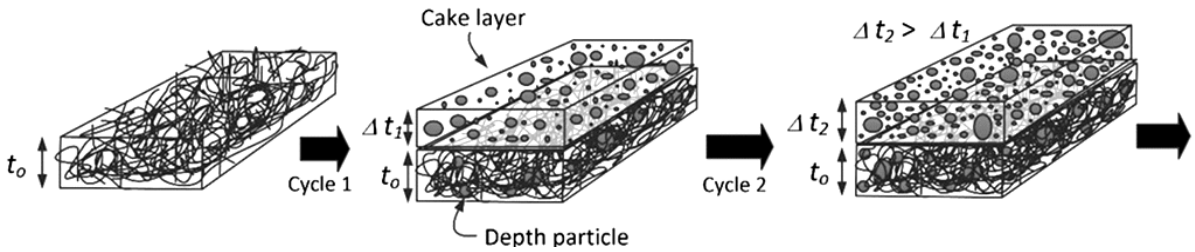

Fig. 2 — Schematic diagram of cake formation and depth filtration in the nonwoven after each filtration cycle

For each filtration cycle, the available pore characteristics will determine the passage of the unfiltered particles. Although, the porometric analysis is useful to get the mean flow pore size (MFP) and smallest pore size, it is still difficult to obtain the number of pores and their exact sizes. Furthermore, the examination of pores becomes more difficult in the loaded filter due to the presence of impurities (Fig. 2). In order to follow variation in the porous network of the loaded filter, the examination of porosity (free space; ε) is an alternative and meaningful choice. The initial porosity (ε_{f0}) of the nonwoven is only due to fibrous network as given below:

$$\varepsilon_{f0} = 1 - \frac{W_o}{\rho_f t_o} \quad \ldots (4)$$

where W_o is the mass density (kg/m^2); ρ_f, the fibre density (kg/m^3), and t_o, the initial thickness (m). At the end of filtration cycle, there is possibility of both cake formation and depth filtration (Fig. 2). The cake layer will create new porous structure of the filtered particles, while the depth particles will occupy the free space in the fibrous network. If the increase in thickness and weight density after first filtration are Δt_1 and ΔW_1 respectively the porosity created in the additional cake layer (thickness Δt_1) can be expressed as:

$$\varepsilon_{c1} = 1 - \frac{\Delta W_{c1}}{\rho_s \Delta t_i} \quad \ldots (5)$$

where ρ_s is the particle density (kg/m^3); and ΔW_{c1} , the weight density of the deposited cake layer. The mass density of depth particulates (ΔW_{d1}) trapped in the fibrous structure can be obtained by deducting ΔW_{c1} from the total weight ΔW_1, as shown below:

$$\Delta W_{d1} = (\Delta W_1 - \Delta W_{c1}) \quad \ldots (6)$$

Due to presence of these depth particulates, the available porosity in the fibrous structure ε_{f1} will be reduced from its original porosity ε_{f0}, as indicated by following relationship:

$$\varepsilon_{f1} = \varepsilon_{f0} - \frac{\Delta W_{d1}}{\rho_s t_o} = 1 - \left(\frac{W_o}{\rho_f t_o} + \frac{\Delta W_{d1}}{\rho_s t_o}\right) \quad \ldots (7)$$

The total porosity after the end of first filtration cycle (ε_{T1}) is the sum of both, fibrous porosity ε_{f1} and cake porosity ε_{c1}, as shown below:

$$\varepsilon_{T1} = \varepsilon_{f1} + \varepsilon_{c1} \quad \ldots (8)$$

This porosity ε_{T1} will influence the filtration in the second cycle (FE_2). Similarly, the available porosity for the (i+1)th filtration can be expressed as:

$$\varepsilon_{Ti} = \varepsilon_{fi} + \varepsilon_{ci}$$

$$\Rightarrow \varepsilon_{Ti} = 2 - \left(\frac{W_o}{\rho_f t_o} + \frac{\Delta W_{di}}{\rho_s t_o} + \frac{\Delta W_{ci}}{\rho_s \Delta t_i}\right) \quad \ldots (9)$$

where ΔW_{di} and ΔW_{ci} indicate the total mass densities of in-depth particulates and of cake surface respectively, and Δt_i is the change in thickness (equal to cake layer) after i^{th} filtration cycle. Here, we have three new variables ΔW_{ci} , ΔW_{di} and Δt_i to calculate ε_{Ti} for each cycle. However, we can measure only two values, i.e. total weight add-on ΔW_i ($\Delta W_{di} + \Delta W_{ci}$) and Δt_i after each cycle, and therefore it is difficult to calculate ε_{Ti}. As an alternative, the variation in porosity can be related to air permeability whose measurement is possible after each cycle. To sum up all, the FE in the next cycle (i+1) depends on the available porosity ε_{Ti}, which, in turn, depends on ΔW_i and Δt_i . The impact of these variables on the cycle variation of the FE could be examined for more understanding.

3 Results and Discussion

3.1 Porometry Results

The passage of the particles through a filter depends on the porous network of the fibrous material. Therefore, the pore characteristics are

important to understand the filtration behavior of different nonwoven filters. The pore dimension could vary significantly throughout the nonwoven structure. However, the mean flow pore size (MFP) and smallest flow pore size (SFP) are relevant in our case, as they directly influence the entrapment of particulates during filtration. Table 2 shows the results of pore features for different samples. Both SFP and MFP decrease with increase in mass per unit area and needle density of the filter. For an example, the SFP values for samples F1 (400 g/m^2; 210×10^4), F2 (500 g/m^2; 210×10^4) and F3 (600 g/m^2; 210×10^4) are 9.63, 8.31 and 7.62 μm respectively. This is attributed to the availability of more number of fibres with increasing mass per unit area, and hence more possibility of fibre intersections, resulting in the formation of lower pore size. Similarly, the increase in needling density causes more punching to a given fibre mass, more intersections points, and lower MFP. In opposite of above two factors, if the fibre density is increased keeping weight and needing density constant, then the structure results in bigger SFP and MFP. This is due to the availability of lower intersection in the coarser fibres (high denier) compared to finer fibres. Given the same mass and needling density, the number of fibres of coarser denier is comparatively less than the number present for finer fibres, and so lesser intersections points. These results are useful in describing the filtration behaviors of different filters as discussed hereunder.

3.2 Effect of Structural Parameters

Table 3 shows the results of FE (first cycle) of all samples. The range of FE lies from 8.84% to 78.04%. The lowest FE (8.84%) is found in F1 (2.5 denier; 400 g/m^2; 210×10^4 punches/m^2), while the highest efficiency (78.04%) is found in F6 (2.5 denier; 600 g/m^2; 225×10^4 punches/m^2). This is consistent with the MFP values for these samples (Table 2). F1 has the highest MFP (34.47 μm), while F6 has lowest (16.07 μm). It means that the pore radius has the significant effect on the filtration performance. The filtration is a physical phenomenon which primarily involves the entrapment of the particulates in the pore, and there is more chance that the particle gets struck if the pores are smaller. Also the flow pore pressure increases with decrease in pore size (Table 2), which favors slow movement of particulates, and therefore more chance of entrapment and sieving.

To see the effect of individual variables, different samples are selected, keeping one parameter variable and other two at constant level. For example, the F4, F5 and F6 have different mass densities of 400, 500 and 600 g/m^2 respectively but same fibre denier (2.5) and needling density (225×10^4 punches/m^2). It is evident that the FE increases with the increase in mass density. The effect is not linear as the FE is increased by 18.96% (35.27-16.31) when the mass density is changed from 400 g/m^2 to 500 g/m^2 (F4 to F5), while it is increased by 42.77% (78.04-35.27) from 500 g/m^2 to 600 g/m^2 (F5 to F6). Although, the MFS values do not change significantly for F5 (16.76 μm) and F6 (16.07 *μm*), there is more variation in their FE values. Herein, the explanation can be given based on the number of available pores and specific surface area. Although the porometry results do not provide the number of pores or fibre surface area, this adds limitation to porometry method to fully describe pore characteristics. Increasing mass density leads to presence of more number of fibres in the structure; so more fibrous surface area is available for surface staining. Also, more fibres result in more intersections which produces more number of smaller pores for particles entrapment.

Table 2 — Porometry results

Sample code	Smallest pore size (SFP), μm	Mean flow pore size (MFP), μm	Smallest pore pressure bar	Mean flow pore pressure bar
F1	9.63	34.47	0.047	0.013
F2	8.31	29.66	0.055	0.015
F3	7.62	29.13	0.061	0.016
F4	6.31	24.01	0.072	0.019
F5	4.35	16.76	0.105	0.027
F6	4.15	16.07	0.110	0.029
F7	8.31	35.21	0.055	0.013
F8	6.31	27.30	0.072	0.016
F9	6.15	26.14	0.073	0.017

Table 3 — Filtration efficiency in the first cycle of difference samples

Sample code	FAS solution used mL	COD mg/L	Filtration efficiency %
F1	0.85 (0.02)	192.8 (6.19)	8.84 (0.52)
F2	0.94 (0.01)	155.3 (4.82)	19.57 (1.04)
F3	1.18 (0.03)	61.5 (2.54)	64.55 (1.27)
F4	0.92 (0.02)	169.6 (8.16)	16.31 (0.54)
F5	1.04 (0.01)	131.2 (5.06)	35.27 (0.99)
F6	1.31 (0.02)	44.8 (1.16)	78.04 (1.81)
F7	0.88 (0.03)	182.4 (9.62)	10.01 (0.95)
F8	0.96 (0.01)	156.8 (5.06)	22.57 (1.11)
F9	1.24 (0.01)	67.2 (4.52)	66.85 (1.27)

Values in parentheses represent standard error. FAS – ammonium sulphate.

If the fibre denier is increased then the FE decreases (Fig. 3). The FE for the courser fibre (6 denier) is lower as compared to finer fibre (2.5 denier) for the same mass density. For example, FEs are 16.31 and 10.01% respectively for samples F4 (2.5 denier) and F7 (6 denier). This can be explained by the fact that coarser fibre results in larger pore size in the structure compared to finer fibre. The MFP for F4 and F7 samples are 24.01 and 35.21 μm respectively, and SFP are 6.31 and 8.31 μm respectively. Additionally, the use of coarser fibre will have less number of fibres in the structure as compared to the use of finer fibres; so both the number of smaller pores and available surface area will be lesser for coarser fibre than in finer fibre.

Figure 4 shows the effect on FE with increasing the needling density, which shows an increasing trend.

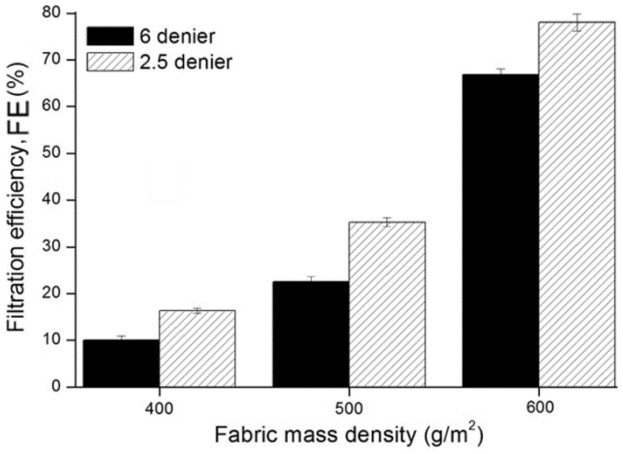

Fig. 3 — Effect of mass density and porosity on the FE

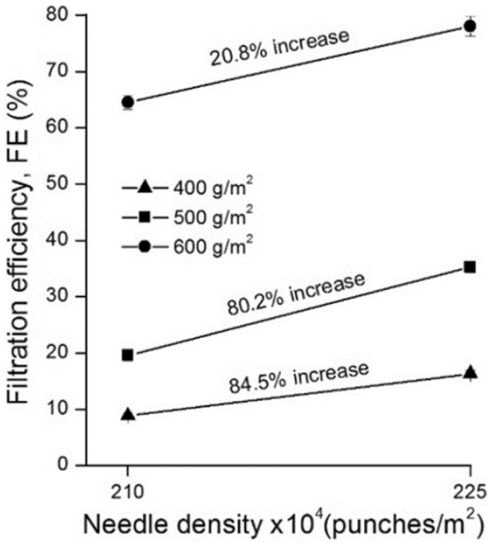

Fig. 4 — Effect of needle density on the FE

More punching action results in more intersection points, and thereby causes reduction in the pore size. For an example, the MFP for F1 (210×10^4 punches/m^2) and F4 (225×10^4 punches/m^2) are 34.47 and 24.01 μm respectively. If we see the percentage change, it is observed that the punching effect is more pronounced for higher mass sample. The percentage change in the FE is 84.5% if we compare F1 and F4 both having mass density 400 g/m^2, while for 600 g/m^2 samples, F3 (210×10^4 punches/m^2) and F6 (225×10^4 punches/m^2), the percentage change in FE is only 20.8%. However, if we compare the absolute value, the achieved FE in F4 is only 16.31% which is still very poor as compared to FE of F6 (78.04%). To conclude, all the above variables have significant effect on the filtration performance ($p<0.01$) (Table 4).

3.3 Repetitive Study

In the earlier section, all the results are based on the first filtration test (FE_1). However, normally, the same filter may be used for repetitive times, and therefore their performance should also be examined for multiple filtration cycles. Figure 5 shows the results of cyclic variation in FE for sample F1. In each filtration test, 500 mL of filtrate is collected and used for the measurement. The FE increases faster for the initial cycles and thereafter it saturates and attains a plateau value [Fig. 5(a)]. Similar trends are also found for the other measured variables including air permeability, thickness (Δt_i) and additional weight (ΔW_i). The decrease in air permeability confirms the reduction in porosity(ε_{Ti}). This finally confirms the negative impact of ε_{Ti} on FE_i. On finding the correlation of the FE with Δt_i and ΔW_i, a strong positive correlation is found. The values of R^2, the coefficient of determination, are 0.98 and 0.99 respectively with Δt_i and ΔW_i.

Similar trends were observed for other samples with high correlation coefficients (> 0.95). Table 5 shows the filtration performance of all samples. The maximum efficiency (FE_{max}) of 84.82% is observed for F6, while the minimum (34.74%) for F1. The

Table 4 — ANOVA analysis to find out significance of different parameters

Source of variation	$F_{calculated}$	$F_{critical}$	p_value
Mass per unit area	1354.68	6.93	0
Fibre denier	103.55	11.26	0
Needling density	158.37	11.26	0

Factors are significant at 99 % confidence interval if p_value is less than 0.01 (FE_1 values were used for the analysis).

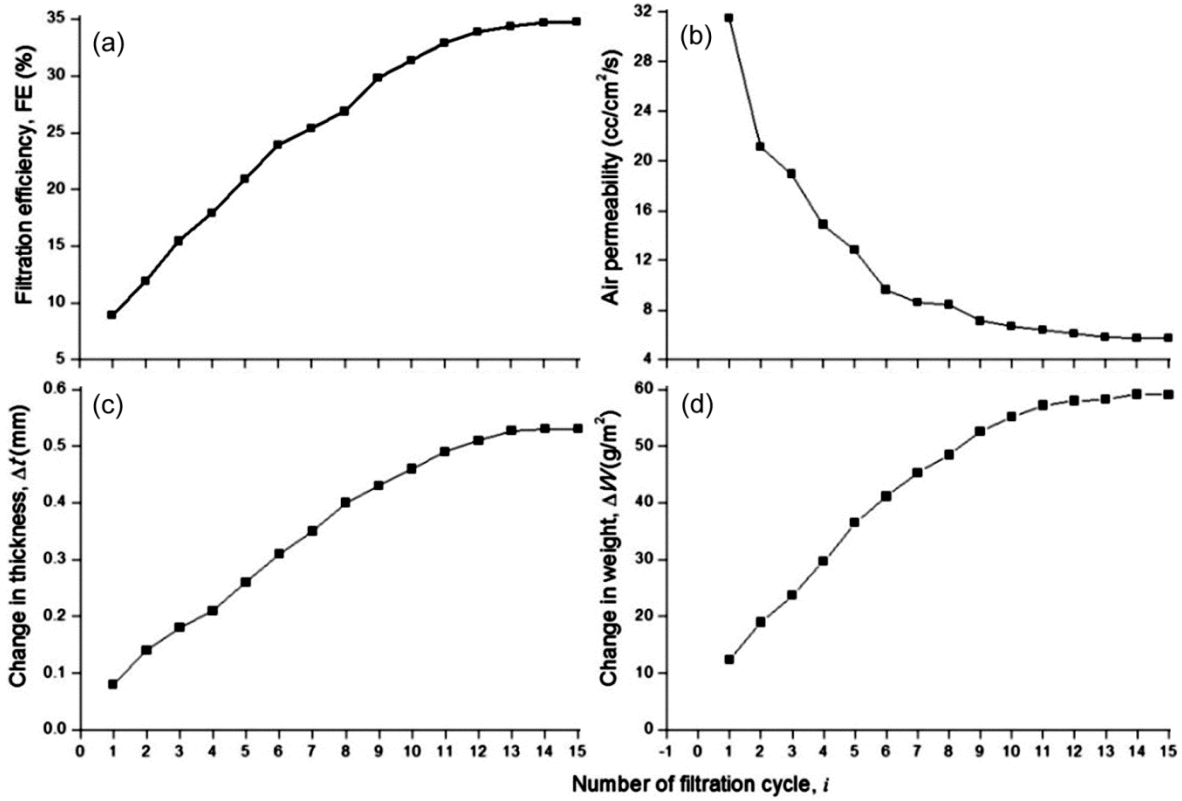

Fig. 5 — Results of cyclic test (a) FE, (b) air permeability, (c) thickness change and (d) weight change

Table 5 — Results of cyclic tests

Sample code	Filtration efficiency (1^{st} cycle, FE_1) %	Maximum filtration efficiency (FE_{max}), %	Total cycles needed to reach saturation (i)
F1	8.84	34.74	14
F2	19.57	43.28	13
F3	64.55	76.54	7
F4	16.31	40.44	12
F5	35.27	52.17	10
F6	78.04	84.82	5
F7	10.01	37.31	13
F8	22.57	48.57	11
F9	66.85	78.43	6

saturation point is different for each specimen, and it ranges from 5 cycles to 14 cycles. F6 and F1 shows minimum (i = 5) and maximum cycles (i = 14) to reach maximum efficiency FE_{max}. The effect of multiple tests is more pronounced for open structure (F1 or F7), showing more than 250% increment in the FE. Despite that, their absolute values are still less than 50%, indicating very poor FE, not suitable for field testing. In contrast, the compact samples (F3, F6 or F9), do not show significant improvement in FE, but their absolute values are comparatively higher than that of open samples (F1 or F7), recommending for their use in water purification.

3.4 Use of Activated Carbon

Although F7 shows 78.04% FE in the first run, but it is still not able to reach maximum efficiency (> 90%) and is incapable of removing very fine particles. This is the inherent characteristics of higher denier sample. Although nanofibres have shown potential in filtering particles smaller than 100nm[6], there is additional issue of high production cost for nanofibres. Surely, the needle-punch sample provides a cheap alternative, and we managed to achieve a fairly good FE; however we still aim to further improve its efficiency before recommending for field testing. The FE of the textile material can also be improved by incorporating activated particles in the structure[16,17]. Activated carbon particles (ACs) are found to be very effective in adsorbing organic and some inorganic material from the contaminated water or air. Herein, we used activated carbon granules (bulk density 40 g/100mL) for the production of activated carbon nonwoven sample (ACs). More specification details of ACs can be found in Table 6. A fixed amount (added weight 100 g of carbon per

Table 6 — Specification for activated carbon (ACs)

Parameter	Value
Water soluble substances	2%
Acid soluble substances	5%
Ash content	0.031%
Bulk density	40 g/100mL
Loss on drying	10% (120º)
Effective mean particle diameter	1.99 mm
Uniformity coefficient	1.21

Table 7 — Improvement in FE of activated carbon nonwoven samples

Fabric code	Filtration efficiency (FE_1), %	
	Without ACs	With ACs
F1	8.84	39.03
F3	64.55	81.72
F6	78.04	95.21
F9	66.85	85.43

1000 cm^2) of the granules of the ACs is placed in the carded web just before the needling process of the nonwoven production. We mainly selected compact structures (F3, F6 & F9) as they show much better initial efficiency (FE_1) as compared to others (Table 5). Table 7 shows the FE*s* of the bare specimens and their counterpart activated carbon specimens. After the addition of ACs, we would be able to reach efficiency up to 95% (F6), much better to be used in real application.

There are several issues still need to be researched before using them as a potential filter media. In this work, we primarily focus on the preliminary study of filtration behavior of different nonwovens, and attempt to get best suited fibrous network with good FE. We assessed FE using self-made contaminated water sample. Future testing is required to observe the performance on the real water sample, obtained directly from the pond in villages. Also, the detailed analysis of the filtered water has to be examined, and matched with the health standards of the pure water. Other task is to check the performance of filter media after wiping the cake layer. Also, the shelf life of the filter media has to be examined and the replacement time for the filter has to be determined.

4 Conclusion

A cartridge filter system has been designed as a cheap alternative for the rural population. It has been found that the pore network and its geometry play an important role in assisting the performance of filter media. The porous network is significantly affected by varying fibre linear density, mass per unit area and needle density of the nonwoven. The FE is significantly affected by all the above parameters ($p < 0.01$). Increasing needling density and mass per unit area improve FE. A nonwoven filter composed of thicker fibre results in open porous network, and shows poor FE as compared to nonwovens of finer fibres. On conducting multiple filtration tests, all samples show further increase in the FE. High correlations are found between the FE with the air permeability, weight density and thickness. Finally, a nonwoven structure showing maximum FE has been selected, and its FE is further improved to more than 95% using ACs. Future study is needed on the field testing, quality assurance study of the filtered pond water and checking of the shelf life of the filter.

Acknowledgement

The authors are grateful to the Department of Science and Technology (DST), The Govt. of India for funding this research work under 'Water Research Initiative' Scheme. (DST/TM/WTI/2K15/01G)

References

1 Miller J E, *Review of Water Resource and Desalination Technology – SAND Report* (Sandia National Laboratory USA), 2003, 800.
2 Montefusco AF, *Filtration Separation*, 42(2) (2005) 30.
3 Zhi-Guo M, Feng-lin Y & Xing-wen Z, *Filtration Separation*, 42(5) (2005) 28.
4 Kothari V, Das A & Singh S, *Indian J Fibre Text Res*, 32 (2007) 214.
5 Zhao F, Chen H, Xue G, Jiang Q & Qiu Y, *J Mater Sci*, 48 (22) (2013) 7869.
6 Uppal R, Bhat G, Eash C & Akato K, *Fiber Polym*, 14(4) (2013) 660.
7 Das A, Alagirusamy R & Nagendra K R, *Indian J Fibre Text Res*, 34 (2009) 253.
8 Das A, Alagirusamy R & Nagendra K R, *J Text Inst*, 102(2) (2011) 93.
9 Shim W S & Leea D W, *Indian J Fibre Text Res*, 38 (2013) 132.
10 Midha V K & Mukhopadyay A, *Indian J Fibre Text Res*, 30 **(**2005) 218.
11 Grzybowska-Pietras J & Malkiewicz J, *Fibres Text East Eur*, 15(5&6) (2007) 64.
12 Kothari V, Das A & Sarkar A, *Indian J Fibre Text Res*, 32 (2007) 196.
13 Thangadurai K, Thilagavathi G & Bhattacharyya A, *J Text Inst*, 105(12) (2014) 1319.
14 Ariadurai S A, Potluri P & Whyte I L, *Text Res J*, 69(5) (1999) 345.
15 Pisarevsky A M, Polozova I & Hockridge P, *Russ J Appl Chem*, 78(1) (2005) 101.
16 Davis W T, Kim G D & Perry T C, *Sep Sci Technol*, 36(5&6) (2001) 931.
17 Aber S & Sheydaei M, *Clean–Soil, Air, Water*, 40(1) (2012) 87.